Radiosynthesis of N-^{11}C-Methyl-Taurine–Conjugated Bile Acids and Biodistribution Studies in Pigs by PET/CT

Anna Christina Schacht[1], Michael Sørensen[1,2], Ole Lajord Munk[1], and Kim Frisch[1]

[1]Department of Nuclear Medicine and PET Center, Aarhus University Hospital, Aarhus, Denmark; and [2]Department of Hepatology and Gastroenterology, Aarhus University Hospital, Aarhus, Denmark

During cholestasis, accumulation of conjugated bile acids may occur in the liver and lead to hepatocellular damage. Inspired by our recent development of N-^{11}C-methyl-glycocholic acid—that is, ^{11}C-cholylsarcosine—a tracer for PET of the endogenous glycine conjugate of cholic acid, we report here a radiosynthesis of N-^{11}C-methyl-taurine–conjugated bile acids and biodistribution studies in pigs by PET/CT. **Methods:** A radiosynthesis of N-^{11}C-methyl-taurine–conjugated bile acids was developed and used to prepare N-^{11}C-methyl-taurine conjugates derived from cholic, chenodeoxycholic, deoxycholic, ursodeoxycholic, and lithocholic acid. The lipophilicity of these new tracers was determined by reversed-phase thin-layer chromatography. The effect of lipophilicity and structure on the biodistribution was investigated in pigs by PET/CT using the tracers derived from cholic acid (3α-OH, 7α-OH, 12α-OH), ursodeoxycholic acid (3α-OH, 7β-OH), and lithocholic acid (3α-OH). **Results:** The radiosyntheses of the N-^{11}C-methyl-taurine–conjugated bile acids proceeded with radiochemical yields of 61% (decay-corrected) or greater and radiochemical purities greater than 99%. PET/CT in pigs revealed that the tracers were rapidly taken up by the liver and secreted into bile. There was no detectable radioactivity in urine. Significant reflux of N-^{11}C-methyl-taurolithocholic acid into the stomach was observed. **Conclusion:** We have successfully developed a radiosynthesis of N-^{11}C-methyl-taurine–conjugated bile acids. These tracers behave in a manner similar to endogenous taurine–conjugated bile acids in vivo and are thus promising for functional PET of patients with cholestatic diseases.

Key Words: taurine conjugation; primary and secondary bile acids; lipophilicity; enterohepatic circulation; cholestasis

Bile acids, the end products of cholesterol metabolism, are formed in the liver and secreted into bile where their total concentration exceeds that of any other metabolite. They play an essential role in the biliary excretory function of the liver, in intestinal dietary lipid absorption, and in metabolic signaling (*1–5*). Human bile contains mainly the primary bile acids, cholic acid (CA) and chenodeoxycholic acid (CDCA), formed from cholesterol in the hepatocytes, but also secondary bile acids such as deoxycholic acid (DCA), ursodeoxycholic acid (UDCA), and lithocholic acid (LCA) formed by transformation of the primary bile acids by colonic bacteria. Before secretion from the hepatocytes, all bile acids are conjugated with glycine or taurine at their terminal side chain carboxylic acid group. Although affected by diet and certain cholestatic liver diseases, glycine conjugates dominate in humans (*6,7*), whereas taurine conjugates dominate in many other species (*8,9*). Conjugation increases the polarity and hence decreases the lipophilicity (lipophilicity = hydrophobicity – polarity) of the bile acids, particularly in the case of conjugation with taurine because of its intrinsically stronger sulfonic acid group compared with the carboxylic acid group of glycine. The lipophilicity of conjugated bile acids is also affected by differences in hydrophobicity dictated by the number and configuration (α or β) of hydroxyl groups (-OH) on the steroidal backbone.

Virtually all conjugated bile acids are recovered at the terminal ileum and returned to the liver with portal circulation. At the sinusoidal membrane of hepatocytes, they are taken up mainly by the Na$^+$-taurocholate cotransporting polypeptide (NTCP), whereas their biliary secretion is governed by the bile salt export pump (BSEP) located at the canalicular membrane of hepatocytes (*10*). BSEP constitutes the rate-limiting step of the overall bile acid transport across hepatocytes and has a high affinity for taurine- and glycine-conjugated bile acids, with the highest affinity for the former (*11,12*). Impairment of BSEP is associated with inherited cholestatic liver diseases including progressive familial intrahepatic cholestasis type 2 and benign recurrent intrahepatic cholestasis type 2 and in acquired forms of cholestasis such as intrahepatic cholestasis of pregnancy and drug-induced liver injury (*13*).

To study the hepatic transport of conjugated bile acids in vivo, we recently developed N-^{11}C-methyl-glycocholic acid (^{11}C-MGCA)—that is, ^{11}C-cholylsarcosine (^{11}C-CSar) (*14,15*). ^{11}C-MGCA is a synthetic analog of the endogenous glycine conjugate of CA, that is, glycocholic acid (GCA). Despite the additional methyl-group, ^{11}C-MGCA behaves in a manner similar to GCA and has proven to be a suitable PET tracer for cholestatic conditions (*16–18*). The only significant (and beneficial) difference caused by the N-methyl-group, is that ^{11}C-MGCA, unlike endogenous bile acid conjugates, is stable toward deconjugation and dehydroxylation by colonic bacteria. Here we report a radiosynthesis of N-^{11}C-methyl-taurine–conjugated bile acids and present 5 novel N-^{11}C-methyl-taurine conjugates derived from primary and secondary bile acids of different lipophilicity (Fig. 1) (*15*). We also report results of PET/CT studies of biodistribution in pigs and dosimetry calculations for the structurally different tracers ^{11}C-MTCA (N-^{11}C-methyl-taurocholic acid), ^{11}C-MTUDCA (N-^{11}C-methyl-tauroursodeoxycholic acid), and ^{11}C-MTLCA (N-^{11}C-methyl-taurolithocholic acid), with ^{11}C-MTCA (3α-OH, 7α-OH, 12α-OH) and ^{11}C-MTUDCA
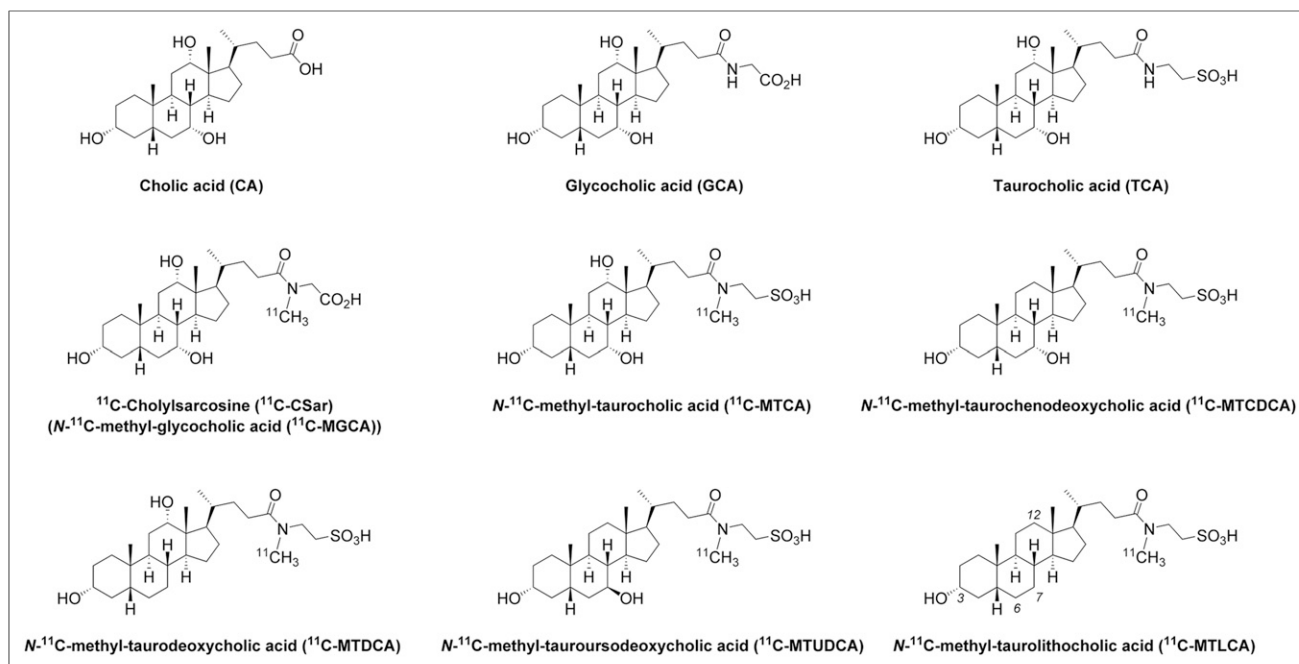
FIGURE 1. Chemical structures of N-^{11}C-methyl-glycine and N-^{11}C-methyl-taurine–conjugated bile acid tracers. For comparison, structures of endogenous CA, GCA, and TCA are also shown.

(3α-OH, 7β-OH) being the least lipophilic and ^{11}C-MTLCA (3α-OH) being the most lipophilic of the developed tracers.

MATERIALS AND METHODS

Chemicals

CA, CDCA, DCA, UDCA, LCA, GCA sodium salt hydrate, TCA sodium salt hydrate, taurine, 1,2,2,6,6-pentamethylpiperidine (PMP), diethyl phosphoryl cyanide (DEPC), and anhydrous dimethylsulfoxide (DMSO) were obtained from Sigma-Aldrich and used as received. Non-radioactive MTCA, N-methyl-taurochenodeoxycholic acid (MTCDCA), N-methyl-taurodeoxycholic acid (MTDCA), MTUDCA, and MTLCA were prepared as described in the supplemental data (available at http://jnm.snmjournals.org). Nonradioactive MGCA, that is, cholylsarcosine (CSar), was prepared as described previously (*14*). The sodium and potassium salts of taurine were prepared by treating taurine with 1 equivalent of aqueous NaOH or KOH, respectively, followed by evaporation of the solvent and oven-drying. European Pharmacopoeia–grade acetonitrile and analytic-grade methanol, NaOH (solid), KOH (solid), and glacial acetic acid were obtained from VWR International Ltd. and used as received. Water (sterile), saline (sterile), ethanol (sterile), and 70 mM aqueous NaH_2PO_4 (sterile, pH 4.5) were obtained from the pharmacy at Aarhus University Hospital. Sep-Pak C8 Plus Short Cartridges (400 mg sorbent/cartridge, 37–55 μm particle size) were obtained from Waters

and preconditioned before use with 10 mL of sterile ethanol followed by 10 mL of sterile water.

Radiosynthesis of N-^{11}C-Methyl-Taurine–Conjugated Bile Acids

The N-^{11}C-methyl-taurine–conjugated bile acids were prepared by a 2-step 1-pot radiosynthesis (Fig. 2): the radionuclide was produced by the $^{14}N(p,α)^{11}C$ nuclear reaction using an IBA Cyclone 18/18 cyclotron. The applied target gas mixture (N_2 with 0.5% O_2) was bombarded at 30 μA for 15–30 min to yield $^{11}C\text{-}CO_2$. The $^{11}C\text{-}CO_2$ was delivered to the synthesis system (Tracerlab FXcPro; GE Healthcare) and converted to $^{11}C\text{-}CH_4$ for further gas phase reaction with molecular iodine to $^{11}C\text{-}CH_3I$. Fifteen minutes after the end of bombardment, the $^{11}C\text{-}CH_3I$ was released from the Porapak N at 190°C and transferred to the reactor of the synthesis system preloaded with a solution of the oven-dried precursor taurine sodium salt (1 mg) dissolved in anhydrous DMSO (300 μL). The $^{11}C\text{-}CH_3I$ was slowly bubbled through the precursor solution (helium flow, 15 mL/min) until maximum activity was trapped in the reactor. The ^{11}C-methylation of taurine was achieved by heating at 80°C for 3 min to give N-^{11}C-methyl-taurine. After the reactor was cooled to 65°C, freshly prepared solutions of the bile acid (12 mg) and PMP (5 μL) in anhydrous DMSO (200 μL), and DEPC (5 μL) in anhydrous DMSO (100 μL) were added successively through dry tubing directly into the reactor solution of
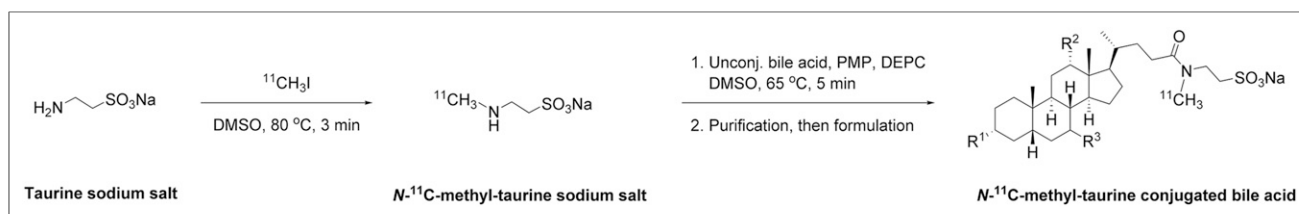

FIGURE 2. Radiosynthesis of N-^{11}C-methyl-taurine–conjugated bile acids (R^1, R^2 = H or α-OH; R^3 = H, α-OH or β-OH).

N-^{11}C-methyl-taurine. The coupling reaction was allowed to proceed for 5 min at 65°C before quenching the reaction with sterile 20% aqueous ethanol (0.7 mL). The crude reaction mixture was purified by preparative reversed-phase high-pressure liquid chromatography using a Synergi Hydro-RP column (4 μm, 21.2 × 100 mm; Phenomenex) and with 30%–40% acetonitrile in sterile 70 mM aqueous NaH_2PO_4 buffer (pH 4.5) as the mobile phase (flow, 15 mL/min; λ = 220 nm). The fraction containing the N-^{11}C-methyl-taurine–conjugated bile acid (retention time, 5–10 min) was collected and diluted with 50 mL of sterile water and then extracted from this solution using a preconditioned C8-catridge. The purified product was eluted from the cartridge using sterile ethanol (1.0 mL) and finally formulated with sterile saline (9.0 mL). Total synthesis time, including ^{11}C-CH_3I production and tracer purification, was 40 min from the end of bombardment.

The radiochemical conversion of the reactions (determined from samples of the crude reaction mixtures) and the identity and radiochemical purity of the isolated N-^{11}C-methyl-taurine bile acid conjugates were determined by liquid chromatography (LC) mass spectroscopy (MS) (LC: Dionex system; MS: Bruker Daltonics HCT Plus ion trap mass spectrometer running in negative ionization mode; the supplemental data provide information for further MS settings) connected in series to a Gabistar radiodetector (Nuclear Interface). The chromatographic column for analysis was a Synergi 4 μm MAX-RP 80A (2.0 × 100 mm; Phenomenex) with 30%–46% acetonitrile in aqueous ammonium acetate (1 mM; pH 3.0, adjusted using glacial acetic acid) as isocratic eluent with a flow of 0.9 mL/min (details are provided in the supplemental data). The chromatographic radio- and MS signals were analyzed using Dionex Chromeleon software (version 6.80) and Bruker Daltonics esquireControl (version 5.3), respectively. The identities of the ^{11}C-labeled bile acid conjugates were confirmed by comparison of retention time and mass spectrum with that of the corresponding ^{12}C bile acid conjugates.

Determination of Lipophilicity by Reversed-Phase Thin-Layer Chromatography

The lipophilicity of MGCA (CSar), MTCA, MTCDCA, MTDCA, MTUDCA, MTLCA as well as GCA, TCA, and CA was determined by reversed-phase thin-layer chromatography (stationary phase, C18; mobile phase, methanol/aqueous ammonium acetate [pH 7.40]) and reported as values of R_{Mw} and S, where R_{Mw} reflects the lipophilicity of the compound— that is, the higher the value of R_{Mw}, the more lipophilic—and S the degree of responsiveness to changes in the mobile phase composition (details are provided in the supplemental data).

PET/CT Biodistribution and Dosimetry in Pigs

Biodistribution and dosimetry was determined in 2 pigs (3-mo-old female Danish Landrace and Yorkshire cross-breed) by PET/CT for ^{11}C-MTCA, ^{11}C-MTUDCA, and ^{11}C-MTLCA after an 18-h fasting with free access to water. The pigs were premedicated with midazolam and s-ketamine; anesthetized with a mixture of midazolam, s-ketamine, and propofol; and mechanically ventilated as previously described (19). A catheter (Cordis) was inserted into the femoral vein for administration of the tracers. Blood pressure; heart rate; body temperature; and arterial blood pO_2, pCO_2, pH, and glucose were monitored continuously and disturbances corrected for by appropriate procedures (19). After completion of the experiment, the animals were euthanized with an overdose of pentobarbital (100 mg/kg). The studies were performed according to the Danish Animal Experimentation Act and the European convention for the protection of vertebrate animals used for experimental and other purposes (European Treaty Series no. 123).

The PET/CT studies were performed with the pigs placed supine in a Siemens Biograph 64 Truepoint PET/CT camera with a 21.6-cm axial PET field of view. A CT scan (250 effective mAs with CARE Dose4D [Siemens], 120 kV, pitch of 1.0, and slice thickness of 2.0 mm) was obtained for definition of anatomic structures and attenuation correction of the PET recordings. Pig 1 (body weight, 41 kg) was administered ^{11}C-MTCA (511 MBq), ^{11}C-MTUDCA (508 MBq), and then ^{11}C-MTLCA (486 MBq), whereas pig 2 (body weight, 36 kg) was administered ^{11}C-MTLCA (536 MBq), ^{11}C-MTCA (571 MBq), and then ^{11}C-MTUDCA (553 MBq). The tracers were administered as intravenous bolus injections, and at least 7 physical half-lives of the ^{11}C radioisotope (half-life, 20.4 min) were allowed to pass between each administration. After administration of the tracer, 6 whole-body PET scans, each with 6 bed positions, were obtained with 3 min between scans and with a progressive increase in scan duration per bed position of 1, 1, 1.5, 2, 3, and 5 min. Thus, each whole-body scan was started 1, 10, 19, 30, 45, and 68 min after tracer injection. Whole-body images were reconstructed using 3-dimensional ordered-subset expectation maximization with 6 iterations and 21 subsets and a 2-mm Gauss filter. All tissues were visually inspected, and organs with accumulation of tracer above that of surrounding tissue were defined as source organs. These organs were liver tissue, gallbladder contents, stomach contents, and small intestine contents. No measurable radioactivity was observed in other organs including kidneys and urinary bladder; urine samples verified that no tracer was excreted in urine. Volumes of interest were manually drawn in each source organ to encompass all radioactivity of the respective organs. Intrahepatic

TABLE 1
Radiochemical Data from Preparation of N-^{11}C-Methyl-Taurine–Conjugated Bile Acids

Tracer	Radiochemical conversion*	Radiochemical yield[†] (not decay-corrected)	Radiochemical yield[†] (decay-corrected)	Isolated radioactivity[‡]	Radiochemical purity[¶]
[11]C-MTCA	78% ± 5%	30% ± 4%	71% ± 7%	5.0–5.8 GBq	>99%
[11]C-MTCDCA	75% ± 4%	26% ± 3%	68% ± 4%	4.7–6.4 GBq	>99%
[11]C-MTDCA	77% ± 2%	25% ± 4%	61% ± 8%	2.2–6.2 GBq	>99%
[11]C-MTUDCA	77% ± 4%	25% ± 3%	66% ± 6%	2.5–6.0 GBq	>99%
[11]C-MTLCA	77% ± 6%	22% ± 1%	65% ± 7%	1.9–4.5 GBq	>99%

*Radiochemical conversion (mean ± SD, n = 3–5) was estimated from LC-radio-MS analysis of crude reaction mixture.

[†]Radiochemical yield (mean ± SD, n = 3–5) is based on amount of isolated radioactivity after purification and relative to amount of ^{11}C-methyl iodide initially trapped in reactor.

[‡]Isolated radioactivity amount of purified product (n = 3–5).

[¶]Radiochemical purity was determined by LC-radio-MS analysis of final product formulation (n = 3–5).
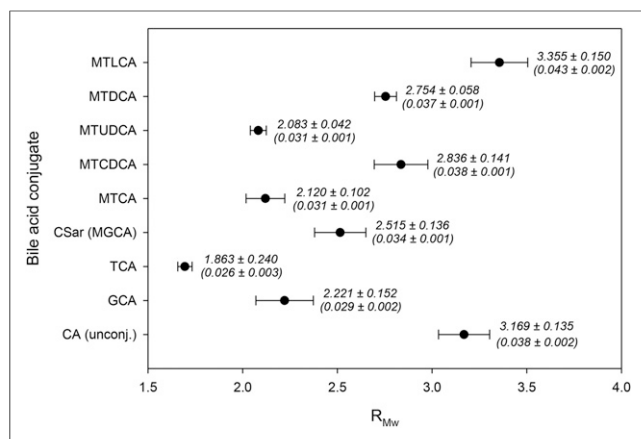
FIGURE 3. Lipophilicity of conjugated bile acids determined by reversed-phase thin-layer chromatography eluting with methanol/aqueous ammonium acetate (pH 7.40). Values of R_{Mw} and S (parentheses) are reported as mean ± SD ($n = 3$).

bile ducts were included in the volume of interest of the liver, whereas the choledochus was included in the volume of interest of the small intestines.

For each source organ, the time course of the non–decay-corrected total radioactivity was extracted and recalculated into time courses of percentage injected dose using injected dose, organ masses, organ densities, and total weight for the reference adult man (*20*). Residence times were computed using the trapezoidal integration method to calculate the area under the curves assuming only physical decay after the last scan, without further biologic clearance. The remainder fraction was calculated by subtracting the individual source organ residence times from the total-body residence time (without voiding), which for ¹¹C is 0.49 h. Residence times for source organs and remainder were used in OLINDA/EXM 1.0 (*21*) to compute organ doses using the male reference phantom and to obtain an effective dose estimate according to International Commission on Radiological Protection publication 60 (*22*).

RESULTS

Radiochemistry

The *N*-¹¹C-methyl-taurine–conjugated bile acids ¹¹C-MTCA, ¹¹C-MTCDCA, ¹¹C-MTDCA, ¹¹C-MTUDCA, and ¹¹C-MTLCA

(1.9–6.4 GBq; Table 1) were prepared with high radiochemical conversion (75%–78%), good radiochemical yield (22%–30%; not decay-corrected), excellent radiochemical purity (>99%), and specific activities in the range of 30–55 GBq/µmol. No protection of the sulfonic acid group of taurine or the hydroxyl groups of the parent bile acids was needed. During optimization of the radiosynthesis, we found that moisture significantly affected the radiochemical conversion of the reaction. The results presented in Table 1 are all based on reactions performed using an oven-dried taurine precursor, dry DMSO, fresh PMP, and fresh DEPC (less than 3 mo old) as well as a rigorously dried synthesis system. If these precautions were not taken, the radiochemical conversion generally dropped to approximately 50%.

Lipophilicity

R_{Mw} values for nonradioactive MGCA (CSar), MTCA, MTCDCA, MTDCA, MTUDCA, and MTLCA are reported in Figure 3. For comparison, the lipophilicity of GCA, TCA, and unconjugated CA was also determined. Values of S are reported in Figure 3 in parentheses. As expected, conjugation significantly decreased the lipophilicity of the bile acids. In addition, taurine conjugates were less lipophilic than glycine conjugates, that is, $R_{Mw}(CA) > R_{Mw}(GCA) > R_{Mw}(TCA)$, whereas a methyl group on the amide nitrogen of a conjugated bile acid slightly increased the lipophilicity, that is, $R_{Mw}(MGCA) > R_{Mw}(GCA)$ and $R_{Mw}(MTCA) > R_{Mw}(TCA)$, although not compensating for the decreased lipophilicity due to conjugation. The results in Figure 3 also show that the number and configuration of hydroxyl groups on the parent bile acid significantly influence the lipophilicity and give rise to the following ranking of the *N*-methyl-taurine–conjugated bile acids: $R_{Mw}(MTLCA) > R_{Mw}(MTCDCA) \approx R_{Mw}(MTDCA) > R_{Mw}(MTCA) \approx R_{Mw}(MTUDCA)$, which corresponds to that of endogenous taurine–conjugated bile acids (*23*).

Biodistribution and Dosimetry in Pigs

PET/CT revealed a similar biodistribution pattern for ¹¹C-MTCA, ¹¹C-MTUDCA, and ¹¹C-MTLCA in the pigs. Figure 4 shows whole-body PET/CT images recorded 1, 10, 19, 30, 45, and 68 min (start of scan) after administration of ¹¹C-MTCA in pig 2. The images show that the tracer is rapidly taken up by the liver and secreted into bile. After secretion into the small intestines, the tracer returns to the liver as a result of enterohepatic recirculation (Fig. 4, 68–98 min). Further whole-body PET/CT images of the tracers in the 2 pigs and the time–activity-curves used for dosimetry calculations are provided in the supplemental data.

Dosimetry data for ¹¹C-MTCA, ¹¹C-MTUDCA, and ¹¹C-MTLCA are presented in Table 2 together with data for ¹¹C-MGCA (¹¹C-CSar) previously published (*14*). Only organs receiving the highest doses are presented in this table. The supplemental data provide a full list of organs. The small intestine and stomach wall were identified as critical organs. The varying distribution of the tracers in the small intestines and gallbladder is considered to reflect the normal physiologic distribution of bile acids. The calculated effective doses were 4.4 ± 0.2, 5.5 ± 0.2, and 8.3 ± 0.9 µSv/MBq for
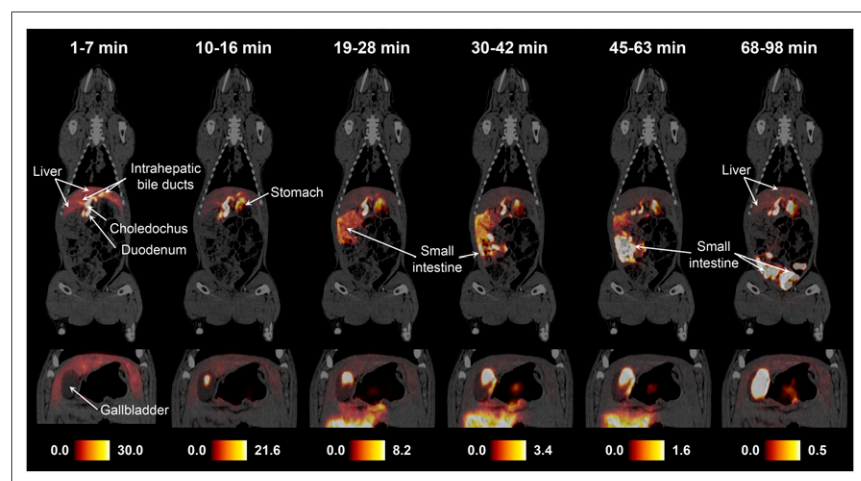

FIGURE 4. Whole-body PET/CT images (coronal view) recorded successively after intravenous bolus administration of ¹¹C-MTCA (571 MBq) in pig 2. Insets are for same respective time intervals but different slice to illustrate content of gallbladder. Color scales are in MBq/mL.

TABLE 2
Absorbed Dose Estimates for ^{11}C-MTCA, ^{11}C-MTUDCA, ^{11}C-MTLCA, and ^{11}C-MGCA*

Target organ	^{11}C-MTCA† (µGy/MBq)		^{11}C-MTUDCA† (µGy/MBq)		^{11}C-MTLCA† (µGy/MBq)		^{11}C-MGCA‡ (µGy/MBq)
	Pig no. 1	Pig no. 2	Pig no. 1	Pig no. 2	Pig no. 1	Pig no. 2	
Gallbladder wall	5.4	31.1	22.0	17.3	5.1	4.5	59.4
Small intestine	34.3	36.4	41.1	32.1	19.6	15.0	39.3
Stomach wall	13.0	11.8	3.5	3.4	53.2	38.0	3.9
Liver	19.5	13.4	15.7	11.8	13.7	11.2	10.8
Total body	2.9	2.8	2.9	2.9	2.7	2.7	2.8
Effective dose (µSv/MBq)	5.6	5.3	4.6	4.2	9.2	7.3	4.4

*Data were obtained from PET/CT biodistribution of tracers in pigs (36–41 kg) and extrapolated to 74-kg human data.
†Biodistribution of tracers was investigated in 2 independent pigs and in different order.
‡Data for ^{11}C-MGCA (^{11}C-CSar) are from Frisch et al. (14).

[11]C-MTUDCA, ^{11}C-MTCA, and ^{11}C-MTLCA, respectively. The effective dose for ^{11}C-MGCA (^{11}C-CSar), approximately 4.4 µSv/MBq, was similar to that of ^{11}C-MTUDCA and ^{11}C-MTCA. The large difference between ^{11}C-MTLCA and the other tracers was due to a significantly higher dose received by the stomach wall when the pigs were administered ^{11}C-MTLCA.

DISCUSSION

As part of an ongoing program on in vivo quantification of hepatic transport of conjugated bile acids by PET (14), we here report the development of a radiosynthesis of N-^{11}C-methyl-taurine–conjugated bile acids (15) and present 5 ^{11}C-labeled conjugates derived from common primary and secondary bile acids.

In humans, only about 5% of the bile pool is from de novo synthesis in the liver; the remaining part recirculates in the enterohepatic circulation. Both primary and secondary bile acids in the intestine (mostly present as conjugates of glycine or taurine) are taken up from the terminal ileum, brought to the liver via portal circulation, and presented to hepatocytes in the sinusoids. Here, conjugated bile acids are taken up mainly by the NTCP and resecreted into the bile canaliculi mainly by the BSEP (10,24). Although the hepatic uptake of bile acids returning from the intestine is highly efficient, a small portion of bile acids escape uptake and enter the systemic circulation. Bile acids spilled into the system circulation, however, are again brought to the liver by the hepatic artery, which mixes with the portal vein before reaching the sinusoids so the residence time of any bile acid in systemic circulation is only a few minutes (2).

Preliminary results in pigs indicate that Ntcp and Bsep are indeed the main transporters of ^{11}C-MGCA, a tracer analog of endogenous glycocholic acid (14). We expect this to be the case for the ^{11}C-methyl-taurine–conjugated tracers presented here as well. In general, NTCP/Ntcp and BSEP/Bsep in humans, mice, and rats have been shown to have higher affinity for conjugates of dihydroxy bile acids, that is, conjugates of CDCA and DCA, than conjugates of the trihydroxy bile acid CA, and with higher affinity for taurine than glycine conjugates (10–12,25). In particular, the affinity of BSEP for conjugated bile acids can be ranked as TCDCA > TCA > TUDCA > GCA (11). Hence, it is likely that the affinity of this essential bile acid transporter will also be higher for ^{11}C-MTCDCA than for ^{11}C-MGCA.

We expect that the tracers presented here do not metabolize on the time scale of a ^{11}C PET study. It has been shown that non-radioactive MTUDCA (26) and MGCA (27,28) are highly resistant to metabolism in rats, hamsters, rabbits, and humans. Also, no metabolites have been observed for ^{11}C-MGCA in pigs (14). It is the additional N-methyl-group that makes these compounds highly resistant toward deconjugation and dehydroxylation by colonic bacteria. On the basis of the knowledge of the metabolism of endogenous TLCA, however, it is possible that ^{11}C-MTLCA, the most lipophilic of the developed tracers, will be metabolized in humans by esterification with sulfate at its 3-hydroxy group and in rodents also by hydroxylation at carbon 6 or 7 (29).

The biodistribution studies of the 3 N-^{11}C-methyl-taurine–conjugated mono-, di-, and trihydroxy bile acids, ^{11}C-MTLCA, ^{11}C-MTUDCA, and ^{11}C-MTCA, revealed that these tracers, like their endogenous taurine analogs, have the highest concentrations in bile ducts, gallbladder, and small intestines compared with other tissues. The effective doses for the 3 tracers were similar to other ^{11}C-labeled tracers including ^{11}C-MGCA (14). The present doses of approximately 0.5 GBq were used in the pigs to obtain good counting statistics. However, because of the high specificity and the rapid distribution of the tracers, 100 MBq, which is a typical dose for ^{11}C-MGCA in a 70-kg human, will be sufficient to obtain a similar data quality in human studies and lead to effective doses in the range 0.4–0.8 mSv corresponding to approximately 10% of the natural background radiation in Denmark. Interestingly, for ^{11}C-MTLCA we observed a significant amount of radioactivity in the stomach. Thus, the most affected single organ in this case was the stomach wall (53.2 µGy/MBq), which is equivalent to 5.3 mSv for an injection of 100 MBq and below common regulatory dose limits. In healthy persons, little gastroduodenal reflux is observed. However, in patients with disordered gastroduodenal motility or pyloric sphincter dysfunction, reflux may occur (2). This should be kept in mind particularly when administering ^{11}C-MTLCA to such patients, because they would receive a higher radiation dose than patients without these disorders. Also, changes in the biodistribution and effective dose should be anticipated in cholestatic patients for all presented tracers.

CONCLUSION

A 2-step 1-pot radiosynthesis of N-^{11}C-methyl-taurine–conjugated bile acids has successfully been developed and used to prepare the N-^{11}C-methyl-taurine conjugates of CA, CDCA, DCA, UDCA, and LCA with good radiochemical yield and excellent radiochemical

purity. It is known that *N*-methyl-taurine (and *N*-methyl-glycine)–conjugated bile acids, unlike their corresponding endogenous taurine (and glycine) conjugates, are resistant toward biodegradation. The additional *N*-methyl-group makes the novel tracer analogs only slightly more lipophilic than their corresponding endogenous conjugates; their overall ranking according to lipophilicity still corresponds to that of the endogenous conjugates. In addition, biodistribution studies of the 3 structurally different tracers derived from cholic (3α-OH, 7α-OH, 12α-OH), ursodeoxycholic (3α-OH, 7β-OH), and lithocholic (3α-OH) acid have shown that the tracers behave in a manner similar to endogenous taurine–conjugated bile acids in vivo, with no detectable elimination in urine. Effective radiation doses have been determined to be in the range 4.4–8.3 μSv/MBq, similar to other ^{11}C-labeled tracers. We believe that these new *N*-^{11}C-methyl-taurine–conjugated bile acids will prove useful for preclinical tests in animals with a naturally high level of taurine-conjugated bile acids and for detailed studies of patients with intrahepatic cholestatic disorders.

DISCLOSURE

REFERENCES

1. Wagner M, Trauner M. Functions of the liver: excretion. In: Rodés J, Benhamou JP, Blei A, Reichen J, Rizzetto M, eds. *Textbook of Hepatology. From Basic Science to Clinical Practice*. 3rd ed. Oxford, U.K.: Blackwell Publishing Inc.; 2007:290–302.
2. Hofmann AF, Hagey L. Bile acids: chemistry, pathochemistry, biology, pathobiology, and therapeutics. *Cell Mol Life Sci.* 2008;65:2461–2483.
3. Frisch K, Hofmann AF. Biliary secretion. In: Keiding S, Sørensen M, eds. *Functional Molecular Imaging in Hepatology*. Sharjah, UAE: Bentham Science Publishers; 2012:49–75.
4. Li T, Chiang JYL. Bile acid signaling in liver metabolism and diseases. *J Lipids.* 2012;2012:754067.
5. Houten SM, Watanabe M, Auwerx J. Endocrine functions of bile acids. *EMBO J.* 2006;25:1419–1425.
6. Trottier J, Białek A, Caron P, et al. Metabolomic profiling of 17 bile acids in serum from patients with primary biliary cirrhosis and primary sclerosing cholangitis: a pilot study. *Dig Liver Dis.* 2012;44:303–310.
7. Dilger K, Hohenester S, Winkler-Budenhofer U, et al. Effect of ursodeoxycholic acid on bile acid profiles and intestinal detoxification machinery in primary biliary cirrhosis and health. *J Hepatol.* 2012;57:133–140.
8. Hofmann AF, Hagey LR, Krasowski MD. Bile salts of vertebrates: structure variation and possible evolutionary significance. *J Lipid Res.* 2010;51:226–246.
9. García-Cañaveras JC, Donato MT, Castell JV, Lahoz A. Targeted profiling of circulating and hepatic bile acids in human, mouse, and rat using a UPLC-MRM-MS-validated method. *J Lipid Res.* 2012;53:2231–2241.
10. Stieger B. The role of the sodium-taurocholate cotransporting polypeptide (NTCP) and of the bile salt export pump (BSEP) in physiology and pathophysiology of bile formation. In: Fromm MF, Kim RB, eds. *Handbook of Experimental Pharmacology. Drug Transporters.* Vol. 201. Berlin, Germany: Springer; 2011:205–259.
11. Noé J, Stieger B, Meier PJ. Functional expression of the canalicular bile salt export pump of human liver. *Gastroenterology.* 2002;123:1659–1666.
12. Byrne JA, Strautnieks SS, Mieli-Vergani G, Higgins CF, Linton KJ, Thompson RJ. The human bile salt export pump: characterization of substrate specificity and identification of inhibitors. *Gastroenterology.* 2002;123:1649–1658.
13. Kubitz R, Dröge C, Stindt J, Weissenberger K, Häussinger D. The bile salt export pump (BSEP) in health and disease. *Clin Res Hepatol Gastroenterol.* 2012;36:536–553.
14. Frisch K, Jakobsen S, Sørensen M, et al. [*N*-methyl-^{11}C]cholylsarcosine, a novel bile acid tracer for PET/CT of hepatic excretory function: radiosynthesis and proof-of-concept studies in pigs. *J Nucl Med.* 2012;53:772–778.
15. Keiding S, Ott P, Sørensen M, Frisch K, Hofmann AF, inventors; Aarhus University, Region Midtjylland; assignee. Radiolabeled bile acids and bile acid derivatives. International patent application WO 2013/113680 A1. Aug. 8. 2013.
16. Sørensen M, Orntoft NW, Frisch K, Ott P, Keiding S. Hepatobiliary excretion measured by PET/CT using the conjugated bile acid tracer ^{11}C-CSar: first experiences in patients with intrahepatic cholestasis [abstract]. *J Hepatol.* 2013;58(suppl 1):S283.
17. Sørensen M, Frisch K, Mortensen F, Olsen A, Keiding S. Uptake of conjugated bile acids from blood to hepatocytes and subsequent excretion into bile canaliculi measured by [*N*-methyl-^{11}C]cholylsarcosine PET/CT in pigs [abstract]. *Hepatology.* 2012;56(suppl 1):332A.
18. Ørntoft N, Frisch K, Sørensen M, Ott P, Keiding S. Hepatic transport of conjugated bile acids in humans measured by ^{11}C-cholylsarcosine PET/CT [abstract]. *Hepatology.* 2014;60(suppl 1):301A.
19. Sørensen M, Munk OL, Mortensen FV, et al. Hepatic uptake and metabolism of galactose can be quantified in vivo by 2-[^{18}F]fluoro-2-deoxy-galactose positron emission tomography. *Am J Physiol Gastrointest Liver Physiol.* 2008;295:G27–G36.
20. Stabin MG, Siegel JA. Physical models and dose factors for use in internal dose assessment. *Health Phys.* 2003;85:294–310.
21. Stabin MG, Sparks RB, Crowe E. OLINDA/EXM: the second-generation personal computer software for internal dose assessment in nuclear medicine. *J Nucl Med.* 2005;46:1023–1027.
22. International Commission on Radiological Protection. 1990 recommendations of the International Commission on Radiological Protection. Publication 60. New York, NY: Pergamon Press; 1991.
23. Sharma R, Majer F, Peta VK, et al. Bile acid toxicity structure–activity relationships: correlations between cell viability and lipophilicity in a panel of new and known bile acids using an oesophageal cell line (HET-1A). *Bioorg Med Chem.* 2010;18:6886–6895.
24. Alrefai WA, Gill R. Bile acid transporters: structure, function, regulation and pathophysiological implications. *Pharm Res.* 2007;24:1803–1823.
25. Geyer J, Wilke T, Petzinger E. The solute carrier family SLC10: more than a family of bile acid transporters regarding function and phylogenetic relationships. *Naunyn Schmiedebergs Arch Pharmacol.* 2006;372:413–431.
26. Schmassmann A, Hofmann AF, Angellotti M, et al. Prevention of ursodeoxycholate hepatotoxicity in the rabbit by conjugation with *N*-methyl amino acids. *Hepatology.* 1990;11:989–996.
27. Schmassmann A, Angelloti A, Ton-Nu HT, et al. Transport, metabolism, and effect of chronic feeding of cholylsarcosine, a conjugated bile acid resistant to deconjugation and dehydroxylation. *Gastroenterology.* 1990;98:163–174.
28. Schmassmann A, Fehr H, Locher J, et al. Cholylsarcosine, a new bile acid analogue: metabolism and effect on biliary secretion in humans. *Gastroenterology.* 1993;104:1171–1181.
29. Hofmann AF. Detoxification of lithocholic acid, a toxic bile acid: relevance to drug hepatotoxicity. *Drug Metab Rev.* 2004;36:703–722.